Available online at www.sciencedirect.com
ScienceDirect
Computer-Aided Design 38 (2006) 939–953
COMPUTER-AIDED DESIGN
www.elsevier.com/locate/cad

Developing an engineering shape benchmark for CAD models

Subramaniam Jayanti, Yagnanarayanan Kalyanaraman, Natraj Iyer, Karthik Ramani*

Purdue Research and Education Center for Information Systems in Engineering (PRECISE), 585 Purdue Mall, School of Mechanical Engineering, Purdue University, West Lafayette, IN, United States

Received 29 October 2005; accepted 4 June 2006

Abstract

Three-dimensional shape retrieval is a problem of current interest in several different fields, especially in the mechanical engineering domain. There exists a large body of work in developing representations for 3D shapes. However, there has been limited work done in developing domain-dependent benchmark databases for 3D shape searching. We propose a benchmark database for evaluating shape-based search methods relevant to the mechanical engineering domain. Twelve different shape descriptors belonging to three categories, namely: (1) feature vector-based, (2) histogram-based, and (3) view-based, are compared using the benchmark database. The main contributions of this paper are the development of a new engineering shape benchmark and an understanding of the effectiveness of different shape representations for classes of engineering parts. Overall, it was found that view-based representations yielded better retrieval results for a majority of shape classes, while no single method performed best for all shape categories.

Keywords: Shape search; Shape matching; Shape benchmarks; Shape databases; Engineering

1. Introduction

Shape-based retrieval of 3D data has applications in various disciplines such as computer vision [1], artifact searching [2], molecular biology [3], and chemistry [4]. The 3D shape retrieval problem has been widely studied in computer vision and computer graphics communities. Extensive reviews of shape matching methods are available in [5–7,45]. Recently, there has been a lot of interest in shape-based retrieval methods for the mechanical engineering domain [8–17]. Even though a number of shape representation methods are being developed to address this problem, there has been limited effort [41,40] in developing a standard dataset for the engineering domain which can be used to benchmark various shape representations.

1.1. Engineering databases vs. multimedia databases

In the multimedia domain, the Princeton Shape Benchmark (PSB) [20] has become the standard and is being widely used for evaluating various shape representations. The shape repository at AIM@SHAPE (http://shapes.aim-at-shape.net/) [53] also makes several 3D models available for researchers to compare shape matching algorithms. However, the PSB and other multimedia datasets are not well suited for the engineering domain due to the following reasons:

1. **Engineering shapes often have high genus** and are characterized by the presence of features such as holes, tunnels, cavities, ribs, and helixes. The number of such features and their relative positioning are important factors in the resemblance of two shapes [34], unlike multimedia where the overall shape is more important.
2. **The 3D models presented in the PSB have a high level of abstraction.** For example, in the engineering domain, airplanes and chairs will generally be considered as assemblies of individual objects (or parts) rather than gross 3D shapes.
3. **The PSB classifies models primarily on the basis of function, and secondarily based on shape.** Most objects created in the multi-media domain can be classified into a category such as “bed”, “tree” or “airplane”, purely based on their nature or function; however, in the engineering domain the existence of many varieties of semi-standard and one-of-a-type components makes it impossible to give names to objects or to classify them into different functional categories. For example, beds with different geometric shapes are placed in the same category in the PSB (see Fig. 1) because of the similarity in their function. Similarly, it is easy to see that dinosaurs and humans belong to different

* Corresponding author. Tel.: +1 765 494 5725; fax: +1 765 494 0539.
E-mail address: ramani@purdue.edu (K. Ramani).

0010-4485/$ - see front matter © 2006 Published by Elsevier Ltd
doi:10.1016/j.cad.2006.06.007

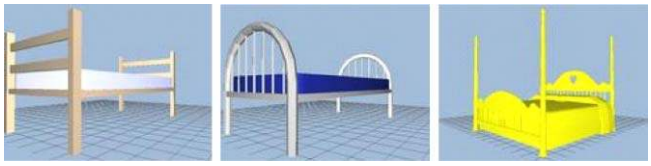

Fig. 1. Parts from the "Beds" category from the PSB [20].

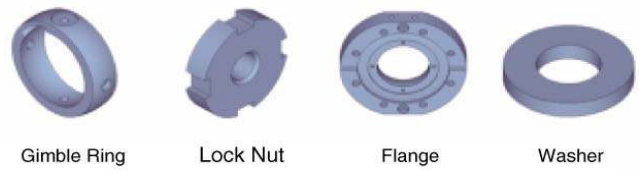

(a) Parts with similar shape but different functions.

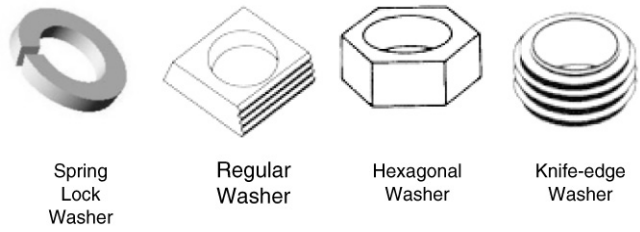

(b) Parts with different shape but same name — washer.

Fig. 2. Examples of parts with different forms and functions.

categories of shapes, but it is more difficult to characterize the shapes in Fig. 2(a) into different categories.

4. **The motivation for experiments with the PSB was only related to multimedia objects.** Shilane et al. [20] explicitly removed all CAD objects from the PSB because their goal was to avoid including domain-independent data.

Consequently, the evaluated shape descriptors may perform differently on an engineering database compared to the PSB. For example, structure-preserving representations in multimedia such as shock graphs [35] and Reeb graphs [36,18, 21,37–39] are widely used and work well for multimedia shapes of Genus-0, but issues related to the topological sensitivity of Reeb graphs have been shown to result in significant number of false positives in engineering databases [18]. Therefore it is necessary to develop benchmark datasets of engineering artifacts, so as to gain better insight into the performance of various shape descriptors for engineering shape retrieval.

In related work, Bespalov et al. [41] provide several classifications for engineering artifacts selected from the National Design Repository (NDR) [11]. This benchmark database consists of four datasets with a total of around 700 models. Among them two datasets, called the Actual Artifacts Dataset (AAD) include: (1) a LEGO®dataset (40 models) and (2) a dataset of 180 models with real-world engineering parts from the NDR. The second dataset consists of two classifications — a functional classification (70 models) and a manufacturing classification (110 models). In our study, we have used both of these datasets, and will henceforth refer to them as the AAD datasets. Details of this dataset are provided in Table 1.

Table 1
Classification of models in AAD

Functional classification	# Models	Manufacturing classification	# Models
Brackets	9	Machined	56
Gears	12	Cast-then-machined	54
Housings	6		
Linkage arms	13	Total	110
Nuts	7		
Screws and bolts	18		
Springs	5		
Total	70		

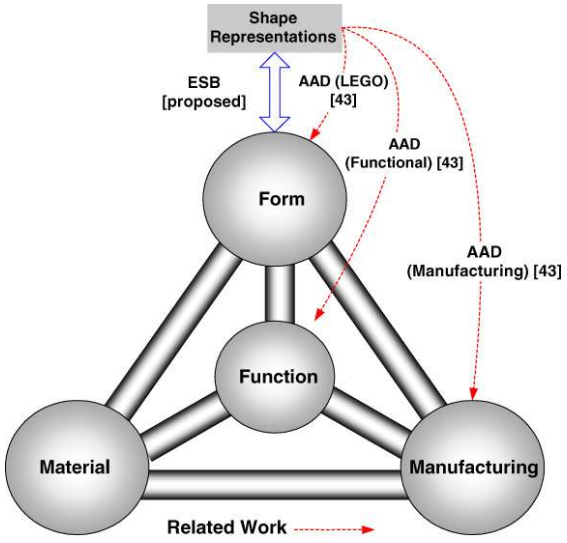

Fig. 3. Shape representations and the elements of product design (adapted from [52]).

1.2. Motivation for an engineering shape benchmark

It is well-known in engineering that product design is an iterative process, and that the different aspects of product design are interdependent. Fig. 3 presents the relationships between various aspects of product design. The form of a product or component includes shape, color, texture, product architecture, and other factors related to the structure of the product [52]. Since shape representations try to approximate the form of an artifact by capturing various shape features, our goal in developing the engineering shape benchmark (ESB) was to determine whether various shape representations have enough shape content in them to discriminate between different forms that we come across in the engineering domain.

For the engineering domain a primarily function-based classification is difficult because parts with different functions may have similar shape (see Fig. 2(a)) and vice versa [51]. For example, gimble rings are used in lighting fixtures for 'fastening'; lock nuts are used primarily for 'locking', while flanges are used for 'connecting' two components. Similarly, the same washer shown in Fig. 2(a) may be used for fastening or thermal insulation depending on where it is used and its

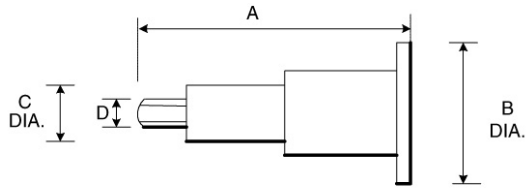

		A	B	C	D
125 T-2	**Disc Pin**	3-1/8"	1-1/2"	1"	5/8"
125 T-3	**Plaiter Stud**	3-5/8"	1"	5/8"	1/2"
125 T-7	**Plaiter Pin**	3-7/8"	1-1/2"	7/8"	5/8"
12853	**Stud**	4"	2"	1-1/2"	7/8"
110256	**Bolt**	4-7/6"	2-3/8"	1-3/8"	1"
110798	**Hinge Pin**	4-1/2"	3"	2"	1-3/8"
23088	**Axle**	4-21/32"	2"	1-1/2"	1"

Fig. 4. Similar parts bearing different names (adapted from [51]).

material properties. One cannot always explicitly state the function of an engineering component purely based on its shape. As a result, designing a function-based classification for the engineering domain using 3D shape representations is a challenge. The AAD functional dataset provides one such classification. However, depending on the requirements of the application, several different classifications are possible for the same set of 3D models. Although all the parts in Fig. 4 (e.g. Disc Pin, Stud, Axle, etc.) are similar in shape, they are given different names depending on context or function. Gombinski [51] suggests that a classification system based on design features is more objective and will make the classification immune to interpretation. Shape-based search systems in the engineering domain should aim to automate appropriate aspects of this process, thereby eliminating subjectivity from classification and retrieval. Similarly, the AAD manufacturing classification dataset classifies artifacts into two categories based on their manufacturing process. However, advances in manufacturing processes and capabilities often tend to blur the mapping between form and the manufacturing method [32]. Increasingly complex shapes can be manufactured in ways that were not thought possible before. As a result, manufacturing classification is also an open research challenge [41].

The classification of 3D models in the engineering shape benchmark (ESB) is designed to overcome these problems. In his classical paper on classification and coding, Gombinski [51] provides an excellent review of the applications of component classification based on shape features, especially in design standardization, inventory control, production planning, and cataloging. The motivation for using a primarily shape-based classification in the ESB is that parts that are similar in their form (a) are easy to modify and reuse in new designs, (b) may have similar manufacturing processes, (c) provide additional insight for design-analysis or manufacturing of similar forms, and (d) can be outsourced to the same supplier.

The ESB dataset contains a total of 867 3D CAD models classified into a number of shape classes. Since function-to-form mapping is not one-to-one, the ESB database is classified into 'shape categories' that are finer than functional categories, i.e. parts within a category are markedly different in form from parts in other categories. Hence, although there is no guarantee that parts in the same category may have the same function or manufacturing process, they share similar shape characteristics.

2. A 3D engineering shape benchmark (ESB)

This section describes the processes of acquiring 3D models for the benchmark database, classification of 3D models and evaluation of shape representations, described in Section 3.

2.1. Model acquisition

The 3D models in the database were acquired from a variety of sources including the National Design Repository [29], websites on the internet [30,31], and industry. In addition, we have included many CAD models created by students in the undergraduate design class at Purdue University. Large commercial repositories of standard parts are also available on the internet. However, one of the major difficulties in building benchmark databases for engineering arises due to the proprietary nature of many engineering designs and their non-availability for public use. Hence we took special care to include such non-standard parts in our collection. This ensures that the 3D models in the ESB span a diverse set of shapes with a significant number of real-world engineering artifacts. We have provided these models for academic research and encourage other researchers to use the ESB for testing new shape matching methods. We will continue to add models to our ESB to encompass a wider variety of shapes and periodically update the existing benchmark.

Each 3D model in the ESB has CAD files in two different neutral formats (STL and OBJ) and an associated thumbnail image (JPG). Models from the ESB can be downloaded along with a classification schema from our website http://purdue.edu/shapelab. Ignoring some small features during conversion from proprietary commercial formats to neutral format led to the introduction of a few duplicates in the ESB.

2.2. Model classification

Users of a shape-based search system are likely to search a database of previous parts with some intent in mind. In order to keep our benchmark database as general as possible, we used the classification methodology developed by Swift and Booker for the purposes of cost estimation and process planning [32] for the base classification. The models for the benchmark database were classified by six individuals unrelated to this research, with varying degrees of training in Mechanical Engineering. We provided these individuals with thumbnail images of 3D models for classification. In case of uncertainty, the respective 3D models were also provided.

Based on the Swift and Booker model, a total of 1391 3D models were initially partitioned into three super-classes, namely:

Table 2
Classification of models in ESB

Flat-thin wall components	# Models	Rectangular-cubic prism	# Models	Solids of revolution	# Models
Backdoors	7	Bearing blocks	7	90 degree elbows	41
Bracket like parts	18	Contoured surfaces	5	Bearling like parts	20
Clips	4	Handles	18	Bolt like parts	53
Contact switches	8	L Blocks	7	Container like parts	10
Curved housings	9	Long machine elements	15	Cylindrical parts	43
Miscellaneous	*12*	Machined blocks	9	Discs	51
Rectangular housings	14	Machined plates	49	Flange like parts	15
Slender thin plates	12	*Miscellaneous*	*21*	Gear like parts	36
Thin plates	23	Motor bodies	7	Intersecting pipes	9
		Prismatic stock	36	Long pins	58
Total	107	Rocker arms	10	*Miscellaneous*	*33*
		Slender links	13	Non-90 degree elbows	8
		Small machined blocks	12	Nuts	19
		T shaped parts	15	Oil Pans	8
		Think plates	12	Posts	11
		Thick slotted plates	20	Pulley like parts	12
		U shaped parts	25	Round change at end	21
				Simple pipes	16
		Total	281	Spoked wheels	15
				Total	479

- *Solids of revolution*: Part envelope is largely a solid of revolution
- *Rectangular–cubic prism or prismatic*: Part envelope is largely a rectangular or cubic prism, and
- *Thin-walled*: Parts with thin-walled sections and shell-like components.

Within each super-class, models were further classified into clusters of similar shapes. A model was included in a particular category only when the six individuals agreed upon it. This classification process continued iteratively until all the 1391 models were exhausted. Initially, a large number of trivial models were removed. Of the remaining models, classes containing less than 4 models which could not be grouped with other classes were moved into the "Miscellaneous" class in the ESB. The final classification consists of 801 models classified into 42 categories of similar parts such as "Discs", "T-shaped parts" and "Bracket-like parts," and 66 models classified into three "Miscellaneous" classes, one in each super-class. A list of super-classes along with their respective classes is shown in Table 2. The naming of the classes has been made in such a way to describe the general shape of parts in that class. The names might have a functional meaning too but that is only incidental.

2.3. Evaluation methodology

We used standard evaluation procedures from information retrieval, namely precision–recall curves and E-measure, for evaluating the various shape representations. We also retrieved models randomly to ensure that every shape representation performed better than random retrievals (RDM). Precision–recall (PR) curves describe the relationship between precision and recall for an information retrieval method. Precision is the ratio of the relevant models retrieved to the retrieval size. Recall is the fraction of the relevant models retrieved for a given retrieval size.

A perfect retrieval retrieves all relevant models consistently at each recall level, producing a horizontal line at precision = 1.0. However, in practice, precision decreases with increasing recall. The closer a PR curve tends to the horizontal line at precision = 1.0, the better the information retrieval method. We used standard techniques of constructing PR curves from the NIST TREC standards [33].

In addition to the PR curves, we present the E-measure for all the methods evaluated here. The E-measure [48,20] provides a single value which describes the performance of the retrieval for a given retrieval size. The user is usually most interested in the first R matches, e.g. fitting onto the first result page. The E-measure incorporates both the precision and recall computed for a fixed number of top k matches:

$$E = \frac{(b^2 + 1)}{\frac{1}{P} + \frac{b^2}{R}} \tag{1}$$

where b indicates the relative importance of precision and recall.

We set $b = 0.5$ and calculate E-measures for a given retrieval size $R = 10$ (or 20), i.e. we assume that 10 (or 20) thumbnail images representing the 3D models appear on a result page. The value of b indicates the weight given to precision and recall, respectively. By choosing a value of 0.5, we are weighting the precision and recall equally. From the above definitions, it follows that the E-measure can range between 0 and 1, and that the higher the E-value, the better the retrieval effectiveness. In our study, we calculated the E-measures for different retrieval sizes.

In addition to the standard measures, we also quantified the performance of shape representation methods with respect to a base method (in our case, 3D shape distributions) as an Average of Differences (AOD) [40]. Although this is not a standard practice in information retrieval, we find that it gives

relevant results in the context of this study. We calculated the AOD between the precision values of 3D shape distributions and the rest of the methods under investigation. This average performance is expressed as a percentage of the performance of the base method.

3. Shape representations

A comprehensive review of various shape representations and search techniques for 3D shapes is available in [5–7]. Based on the type of descriptor used, these methods can be classified into three types [45]: Feature vector-based, histogram-based, and graph-based. We create a separate class in the feature vector-based methods called the view-based methods to help us understand the results clearly. Feature vector (FV) based representations use geometric transformations to obtain shape characteristics while histogram-based representations obtain statistics about angles and distance between points on the surface of the 3D model to represent the global shape of 3D objects. View-based representations obtain multiple 2D views of the 3D object from different orientations and represent their geometry using statistical or 2D shape measures. Examples of FV-based representations include moment invariants, spherical harmonics and crinkliness and compactness, while 3D shape distributions and solid angle shape histograms are representatives of histogram-based methods. Similarly, 2.5D spherical harmonics [22], and 2D Shape Distributions [23,24] are some examples of view-based representations. We briefly describe below the 12 shape representations that we have used for benchmarking.

3.1. Feature vector-based methods

3.1.1. Moment invariants (MI)

The three second-order moment invariants [49,46,47] for the model are stored as a feature vector. Moment invariants are by nature independent of orientation. These values are obtained by calculating the translation, rotational and scale invariant second-order moments for every voxel in the 3D model. For this feature vector, we use the L1 metric as the distance measure. More details can also be found in [6,40].

3.1.2. Principal moments (PM)

The principal moments for a 3D model [49] are the three eigenvalues of the moment matrix M (see Eq. (2)) which is obtained from the second-order moments as given in Eq. (3). More details can be found in [6,40].

$$M = \begin{bmatrix} \mu_{200} & \mu_{110} & \mu_{101} \\ \mu_{110} & \mu_{020} & \mu_{011} \\ \mu_{101} & \mu_{011} & \mu_{002} \end{bmatrix} \rightarrow \begin{bmatrix} \mu_{xx} & 0 & 0 \\ 0 & \mu_{yy} & 0 \\ 0 & 0 & \mu_{zz} \end{bmatrix} \tag{2}$$

$$\mu_{lmn} = \int\int_{-\infty}^{\infty}\int (x-\hat{x})^l (y-\hat{y})^m (z-\hat{z})^n \times \rho(x,y,z)\,\mathrm{d}x\mathrm{d}y\mathrm{d}z \quad l,m,n = 1,2,3,\ldots \tag{3}$$

where $(\hat{x}, \hat{y}, \hat{z})$ is the centroid of the model and where ρ is the density function.

3.1.3. 3D Spherical harmonics (SH)

Spherical harmonics are a decomposition of a spherical function by finding the Fourier transform on a sphere [21]. The theory of spherical harmonics says that any spherical function $f(\theta, \phi)$ can be decomposed as the sum of its harmonics as seen in Eq. (4):

$$f(\theta,\phi) = \sum_{l\geq 0}\sum_{|m|\leq l} a_{lm} Y_l^m(\theta,\phi) \qquad 0 \leq \theta \leq \pi,\ 0 \leq \phi \leq 2\pi \tag{4}$$

where a_{lm} are the Fourier coefficients and $Y_l^m(\theta, \phi)$ are the solutions to the normalized Laplace equation in spherical coordinates. The spherical harmonic coefficients can be used to reconstruct an approximation of the underlying object at different levels. Similar to moments, a partial yet accurate description of the part can be obtained by using a limited subset of Fourier coefficients. Intuitively, we expect this method to perform especially well for objects with radial symmetry, because of the spherical decomposition.

3.1.4. Surface area and volume based attributes

a. *Surface area and volume (SAV)*

In a general shape-based search system, shape representations are required to be independent of translation, rotation and size. However, in the mechanical engineering domain, the surface area and volume of a component have serious implications on the manufacturability of an object. Due to their relevance to design and manufacturing we include these representations in our tests.

b. *Surface area to volume ratio (SVR)*

For the same volume, thin-walled components such as manifolds and tubular parts often have higher surface area compared to prismatic components. Hence the surface area to volume ratio (SVR) will help distinguish between thin-walled and prismatic components and can be used to prune the database when using a multi-step search approach.

c. *Crinkliness and compactness (CC)*

Crinkliness and compactness are two feature vectors developed by Corney et al. [14]. Compactness is defined as the non-dimensional ratio of the volume squared over the cube of the surface area. Crinkliness is defined as the surface area of the model divided by the surface area of a sphere having the same volume as the model.

3.1.5. Geometric ratios (GR)

We have also included the two aspect ratios of the bounding box for a 3D model in our tests due to the simplicity of computation and its relevance to classification. The underlying assumption here is that the aspect ratios will serve as good initial search filters.

3.2. Statistics-based representations

3.2.1. 3D Shape distribution (3DS)

Shape distributions represent the shape signature as a probability distribution sampled from a shape function

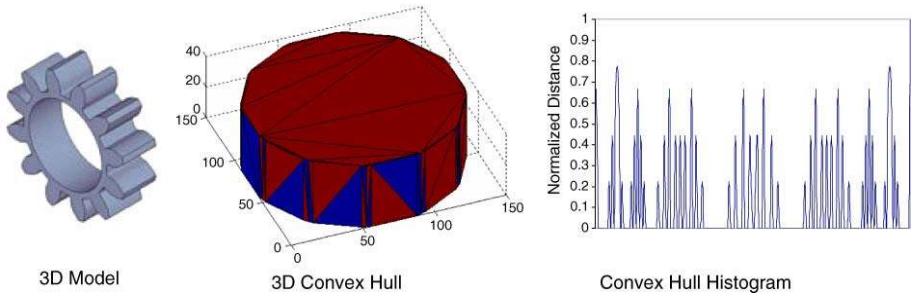

Fig. 5. Procedure of converting a 3D model into the convex hull histogram representation.

measuring the geometric properties of a 3D model [25,19]. In this study, we use the D2 shape measure, as it has been shown to provide the best performance among all other shape distributions.

3.2.2. Convex hull histogram (CHH)

In this shape representation method we compute the 3D convex hull for a given model using the Quickhull [26] algorithm. Then we build a histogram of the pairwise distances based on the points obtained from the convex hull [27,28]. This method is identical to the basic idea described in Rea et al. [50], which presents a detailed study analyzing the merits of this method.

The number of histogram bins is set based on the accuracy needed for similarity searching. We divided the histogram into 200 bins and the values of the histogram bins are normalized and stored in the database for comparison. Models are retrieved based on the L1 norm for similarity searching [28]. Some of the key features of this method are illustrated in Fig. 5. The convex hull only considers the external convex envelope and does not take into account the concave features such as holes and the gear tooth contacts. As a result, the CHH method may serve as a good filter to obtain parts with similar external envelope.

3.2.3. 3D Shape histogram — solid angle (SAH)

The solid-angle-based shape histogram method measures the concavity and the convexity of geometric surfaces. It is described in more detail in [3,16,17]. Histograms are usually based on a complete partitioning of the 3D space into disjoint cells which correspond to the bins of the histograms. The three-dimensional data space is divided into axis-parallel and equi-sized partitions. This kind of space partitioning is especially suitable for voxelized data, as cells and voxels are of the same shape, i.e. cells can be regarded as coarse voxels. Each of these partitions is assigned to one or several bins in a histogram based on different models. We tested a solid-angle-based similarity model as given below.

Let $K_{c,r}$ be a set of voxels that describes a 3D voxelized sphere with central voxel c and radius r. For each surface-voxel $\overline{v}$ of an object o the solid-angle value is computed as follows. The voxels of o which are inside $K_{v,r}$ are counted and divided by the size of $K_{v,r}$, i.e. the number of voxels of $K_{v,r}$. The resulting measure is called the solid-angle value $SA(\overline{v}, r)$ and can be computed as follows:

$$SA(\overline{v}, r) = \frac{|K_{v,r} \cap V^o|}{|K_{v,r}|}. \tag{5}$$

The solid-angle value of each cell is transferred into three bins — surface voxels, inside voxels and no voxels. The histogram represents the 3D shape of the object and the L1 norm is used to determine the similarity between two objects.

3.3. View-based representations

We present an evaluation of three view-based shape representations which have shown promising results in recent experiments on various databases. However, several other two-dimensional view-based approaches have been proposed in the literature, including aspect graphs [45], which were used in computer vision research. For a review of other view-based methods please refer to [5–7].

The view-based methods proposed in this section have some unique advantages compared to the other 3D shape-based techniques. They can not only be applied for 3D model matching but also for matching 3D models with 2D vector drawings, as well as scanned drawings. This is especially useful from an engineering CAD perspective since there is a need to compare 3D CAD models with legacy 2D drawings, which are prevalent in several manufacturing industries.

3.3.1. Light field descriptors (LFD)

Light field descriptors were proposed by Chen et al. [43] and have been shown to perform well on the PSB. The LFD method represents a 3D model as a collection of 2D images rendered from uniformly sampled positions on a viewing sphere located around the model. Each viewing position yields a 2D image representing the silhouette of the 3D object. The 2D views are then described using Zernike moments for the filled contour and the Fourier descriptors for the contour. The distance between two descriptors is defined as the minimum L1-difference, taken over all rotations and all pairings of vertices on two dodecahedra. Comparison between a pair of 3D models is obtained using a cross-correlation measure between the 60 views of each object. We obtained the implementation of the LFD method from the 3D Model Retrieval website at National Taiwan University (http://3d.csie.ntu.edu.tw/). Details of the implementation are described in the accompanying paper [44].

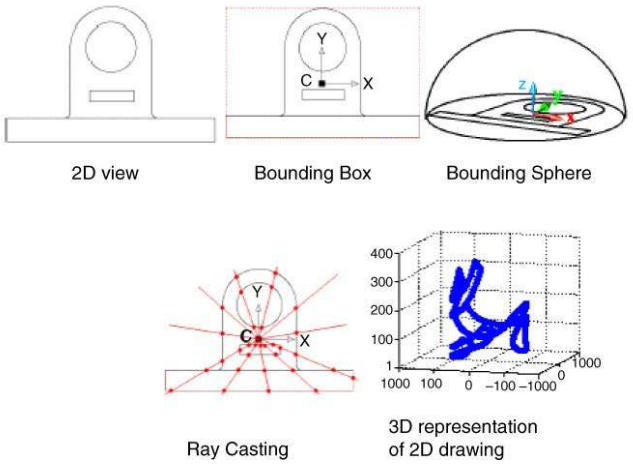

Fig. 6. Procedure of converting a 2D view into the 2.5D harmonics representation.

3.3.2. 2.5D spherical harmonics (2.5DSH)

The 2.5D spherical harmonics technique is a new representation proposed in [23] for representing 2D engineering drawings and 3D models. In this work, a 3D model is first converted into a set of three 2D views through a pose estimation algorithm described in [23,24]. Each 2D view is represented as a spherical function by transforming it uniquely from 2D space into 3D space [42]. The 2D view is initially enclosed in a bounding hemisphere such that the 2D view lies in the equatorial plane of the hemisphere, the radius of the hemisphere is half the length of the diagonal of the bounding rectangle, and the centroid of the hemisphere coincides with the centroid of the bounding rectangle. Subsequently, 2D rays are cast from the centroid through a set of sampled directions which lead to intersections with the edges of the 2D view. The intersection points represent the 2D image. A spherical harmonics transformation is carried out to transform all intersection points $\{p_i = f(\theta_i, d_i)\}$ into a spherical function form $\{p_i = f(\theta_i, \varphi_i, d_i)\}$ by introducing a new variable φ_i. To ensure each intersection point p_i corresponding to a unique (θ_i, φ_i), a simple transformation is used to determine φ_i:

$$\varphi_i = \arctan\left(\frac{d_i}{r}\right). \tag{6}$$

The resulting spherical harmonic transform yields the shape descriptor for the 2D view (see Fig. 6). Thus, the shape matching problem is reduced to several simple steps, such as sampling, normalization, and distance computation between the descriptors.

In our tests we used a bandwidth of 64 for the 2.5D spherical harmonics method, i.e., the descriptor of a drawing contains 64 signatures. The L1 norm is used to compare two descriptors. Given a 3D object, the pair of 2D views which provide the best match (i.e. with the least distance) are called the principal matching views. The other two corresponding pairs are determined likewise. The total distance between two 3D models is obtained through the summation of distances between corresponding view pairs.

3.3.3. 2D Shape distributions (2DSD)

Jiantao and Ramani [23,24] recently also proposed a shape representation method to obtain shape signatures of 3D models after automatically obtaining their three orthogonal main views. Subsequently, a statistics-based approach represents the shape of the 2D views as a distance distribution between pairs of randomly sampled points (Fig. 7). The 2D shape distributions thus obtained are used to compare 3D objects. For ease of understanding we call this method the 2D shape distributions (2DSD), although Ref. [23] terms the method 'Orthogonal Main View'. The L2 norm is used for computing distance between two shape distributions. The best matching pair of views is that pair which produces the least distance, and leads to the first principal matching views. The next best matching pair from the remaining views produces the second principal matching views and so on. The total similarity is obtained by computing the summation of distances from the three principal matching view pairs.

4. Results and discussion

We evaluated the precision at various levels of recall for all the shape representation methods to generate PR curves for the ESB classification. For this database, we found that all shape representation methods performs better than the random retrieval method. Comparisons of the three view-based methods – LFD, 2.5DSH and 2DSD – for the manufacturing and functional classifications from Bespalov et al. [41] are presented in Section 4.1.

4.1. Results on AAD benchmark

For our tests, we downloaded the VRML models provided on the national design repository website (http://www.

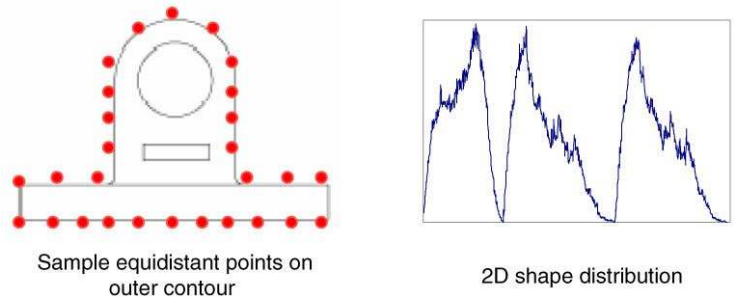

Fig. 7. Procedure for converting a 2D view into the 2D shape distribution representation.

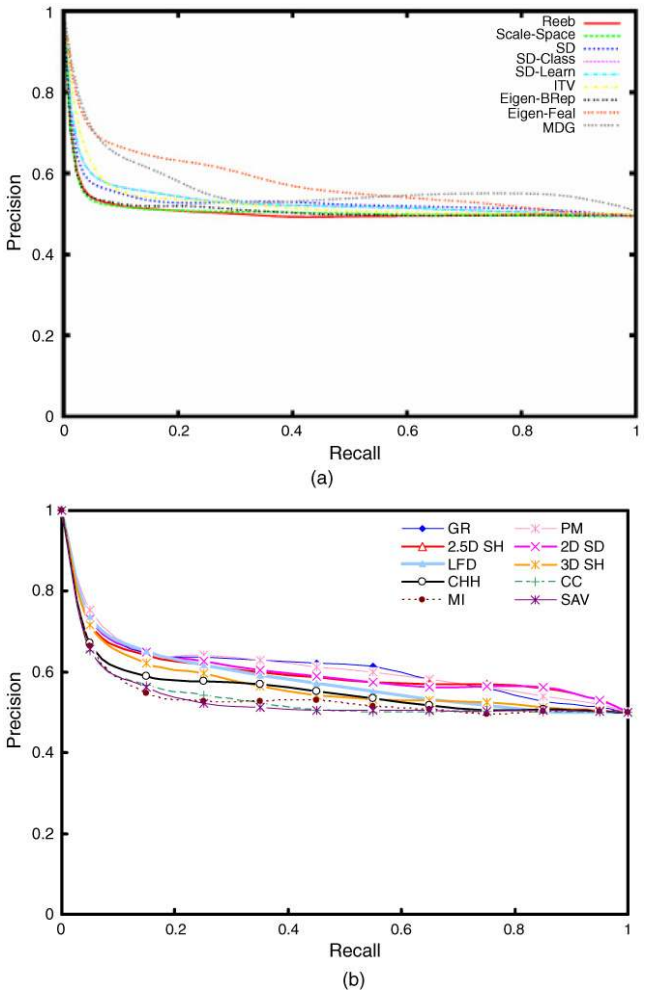

Fig. 8. PR curves for 'Manufacturing Classification' database: (a) for the methods described in Bespalov [41] (figure taken from [41], 2005© ACM Press), and (b) for the methods implemented in this paper.

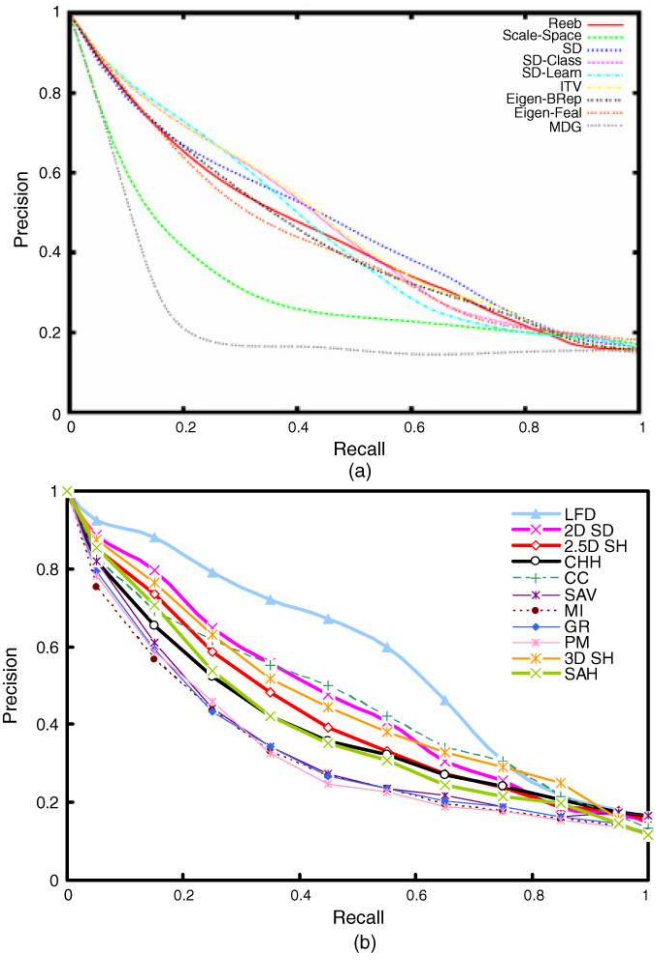

Fig. 9. PR curves for 'Functional Classification' database: (a) for the methods described in Bespalov [41] (figure taken from [41], 2005© ACM Press), and (b) for the methods implemented in this study.

designrepository.org/datasets). We present results for the functional and manufacturing classifications. In their paper, Bespalov et al. [41] presented the precision–recall curves for several methods. Readers are referred to this paper for detailed descriptions of all these methods. We complement those results by presenting the precision–recall curves for several other methods that we described in Section 3. In addition, we also provide the E-measure values for the newly evaluated methods.

4.1.1. Manufacturing classification

Fig. 8(b) presents the new results for the manufacturing classification. In the experimental results presented in [41] it was found that EigenFeat and Eigen-BRep representations, which are derived from the boundary representations (B-Rep) of 3D models, performed better than other methods on the manufacturing classification. From our experiments we also found that the view-based techniques seem to perform well for this classification. The 2.5D SH and 2D SD methods performed better than 3D shape distributions methods at all recall values, while LFD performed well at low and medium recall values.

We expected SAV and CC to perform well on this classification, because of their inclusion of geometric characteristics that are considered in manufacturing decisions, viz., surface area and volume. However, they did not perform well, suggesting that these simple measures may not be enough to distinguish between the two manufacturing processes. An interesting result from our experiments on this dataset is that at medium and high recall levels, simpler shape features, GR and PM, yielded higher precision than even the view-based methods. However, due to the small size of this database and the limited number of classes, it is difficult to draw general conclusions regarding the discrimination characteristics for this classification.

In addition, as noted earlier, none of the currently evaluated shape representations explicitly capture the shape characteristics or manufacturing features that indicate possible manufacturing process.

4.1.2. Functional classification

Fig. 9 presents the results for the functional classification dataset. It was observed that the LFD method performed considerably better than all other methods. The 2.5D SH and 2D SD methods performed comparably with many of the methods evaluated in [41]. At the same time, most of the methods evaluated in our study seemed to perform better than the scale space method, especially at low recall values. Table 3 presents

Table 3
E-measures for the AAD datasets

Functional classification dataset		
Method	E-measure	
	$R = 10$	$R = 20$
LFD	0.563	0.406
CC	0.464	0.429
3DSH	0.456	0.425
2DSD	0.447	0.358
3DSD	0.410	0.330
CHH	0.411	0.360
2.5DSH	0.406	0.340
SAH	0.391	0.314
GR	0.352	0.325
PM	0.318	0.312
SAV	0.303	0.306
MI	0.302	0.277
LEGO®dataset		
Method	E-measure	
	$R = 5$	$R = 10$
SAH	0.559	0.731
GR	0.532	0.641
CHH	0.527	0.613
CC	0.460	0.556
PM	0.420	0.468
LFD	0.452	0.468
SD	0.416	0.455
3DSH	0.434	0.499
SAV	0.429	0.425
MI	0.326	0.394
2DSD	0.348	0.382
2.5DSH	0.320	0.368

E-measures obtained from the 12 shape representations for this dataset. In calculating the E-measure for this dataset, we used retrieval sizes of 10 and 20, since the size of the dataset is 70 and the average group size is 10.

From the E-measure values and the PR curves it is evident that LFD clearly performs better than the other methods. Surprisingly, the CC method also tends to perform better than the other methods, supporting the suggestion that Crinkliness and Compactness measures can be used as initial coarse filters for large databases [14]. For larger retrieval sizes the CC method seems to show better effectiveness than LFD. However, this needs to be confirmed on a larger database, as the number and variety of parts in this dataset is small.

4.1.3. LEGO®Models classification

Fig. 10 presents the results for the LEGO®dataset. The SAH and GR methods performed significantly better than all the other methods for this dataset. Surprisingly, the 2DSD and 2.5DSH methods performed worse than all other methods. Although LFD did not perform as well as GR and SAH, it performed comparably with CC and PM as seen from the E-measures and PR curves. We provided the E-measures for retrieval sizes of 5 and 10 because of the small size of the dataset. Since this dataset consists of 46 models and simple shape measures such as GR and CHH achieve high retrieval rates on this classification, we believe that the results and conclusions are not scalable.

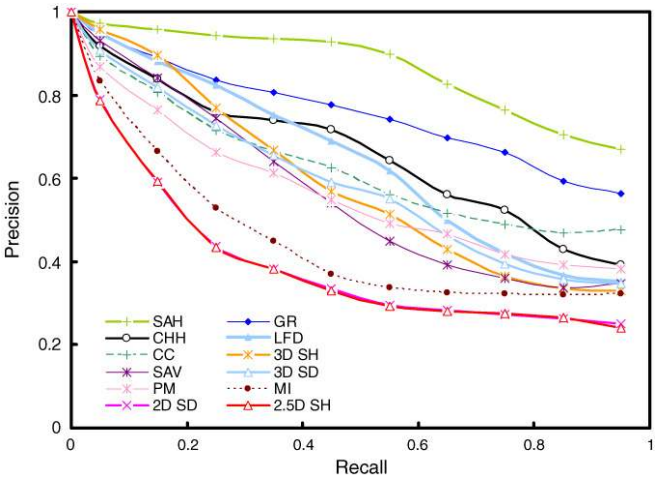

Fig. 10. Comparison of various shape descriptors on LEGO®dataset.

4.2. Results on ESB

Since the AAD datasets are small, we set out to confirm these results on an expanded dataset that encompasses more categories of shapes. Although similar to the LEGO® dataset of [41], the ESB dataset provides one with a comparable, but expanded dataset for performing shape retrieval experiments.

It was found that, on average, the three methods based on 2D views (LFD, 2.5DSH and 2DSD) outperform other methods consistently. Additionally, LFD had significantly better precision than all other methods. These results are consistent with conclusions drawn in [20], where the LFD method works better than other 3D methods. However, as pointed out in [20], view-based methods involve more computation compared to the 3D shape measures such as D2 and SAH. Hence, for quicker comparison, the shape descriptors such as SAV and D2 may serve as good initial filters. On the other hand, the view-based methods bear some resemblance to traditional engineering drawings, which use 2D projections to represent 3D models. Spherical harmonics and the two histogram-based methods – SAH and CHH – also perform better than D2 shape distributions.

Clearly, elaborate histogram-based methods outperform feature vector-based methods such as Moment Invariants and Principal Moments, as observed from Fig. 11. This is because histogram-based methods capture more of the shape content than feature vector-based methods. The only exception is spherical harmonics, which approximates a shape with 64 harmonic coefficients, thereby capturing more shape content than other feature vector-based methods.

On an average, the base method, 3DSD (i.e., D2 shape distribution) method, for AOD performs 5.57 times better than random retrieval. Table 4 shows the AOD of various methods as a percentage value. We have ranked the methods based on their AOD and E-measures. Clearly, the shape representations that hold more shape content are better at retrieving more relevant models. Performing a similar analysis for each of the three

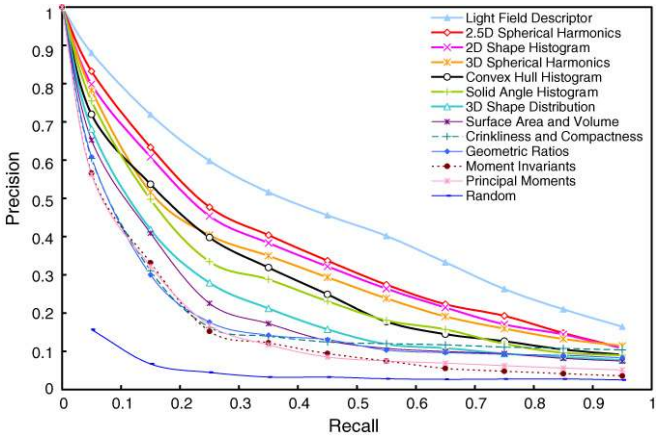

Fig. 11. Precision–recall calculations for 12 shape representations.

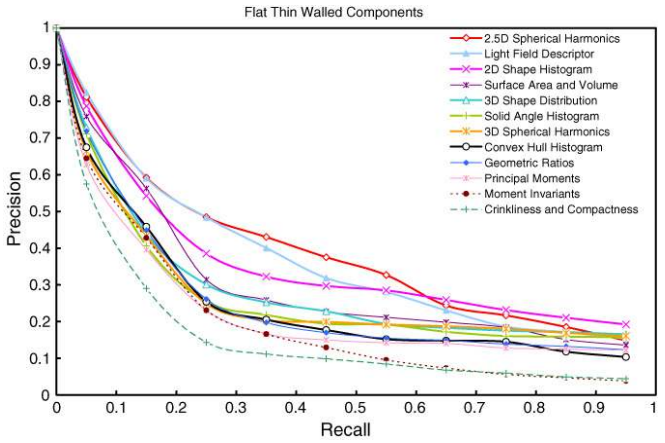

Fig. 12. Precision–recall curves for thin-walled components.

Table 4
Effectiveness measures for 12 shape representations with 3D shape distributions as a reference

Method	E-measure			AOD
	$(R = 10)$	$(R = 20)$	$(R = 32)$	(%)
LFD	0.431	0.406	0.376	143.79
2.5DSH	0.357	0.338	0.303	81.15
2DSD	0.345	0.327	0.296	72.50
3DSH	0.338	0.311	0.288	56.04
SAH	0.312	0.274	0.236	27.00
CHH	0.280	0.243	0.225	33.87
3DSD (D2)	*0.236*	*0.195*	*0.167*	*0.00*
SAV	0.212	0.171	0.149	−13.17
GR	0.208	0.163	0.150	−14.10
CC	0.186	0.161	0.155	−14.38
PM	0.167	0.147	0.137	−35.24
MI	0.168	0.138	0.121	−41.66

super-classes, we found that SAV gives better precision than 3DSD for Thin-Walled parts. Not surprisingly, for all three super-classes, both methods based on 2D views outperformed other methods at low recall levels. The E-measures shown in Table 4 suggest that the trends predicted by the AOD and PR curves are generally true.

4.2.1. Thin-walled components

For the Thin-Walled components class, the view-based methods outperformed other methods. Surprisingly, 3D shape distributions and Surface Area and Volume performed better than the rest of the three methods based on more complex feature vectors, viz., SH, CHH, and SAH. Although simple, the SAV performs better for this super-class because thin-walled components have higher surface areas and lower volume, and these features are more explicitly captured in the SAV compared to other point-based methods. Hence, SAV may serve as a good filter when searching for this super-class of shapes. The PR curves for all the methods for the Thin-Walled components super-class are shown in Fig. 12. This super-class also highlights some of the disadvantages of the LFD method. While the LFD method performs considerably better than the 2.5DSH and 2DSD methods for the other super-classes, it performs comparably with those two methods for this super-class. The differentiating characteristics between the various classes in this super-class come from the internal features such as holes and slots, rather than the external envelope and through holes alone. The LFD method captures these features. Since the 2.5D SH method and 2D SD methods capture these internal features well, they tend to maintain higher precision for large recall values.

4.2.2. Prismatic parts

For this super-class, LFD has considerably high precision for all recall values. In addition, four other methods performed consistently better than D2 shape distributions, namely the three 2D view-based methods (2.5DSH and 2DSD), 3D Spherical Harmonics and SAH. While the 2D view-based methods performed consistently well, two other methods, viz., spherical harmonics (3DSH) and Solid Angle histograms (SAH), performed comparably at higher recall levels (after 0.3 and 0.5 recall respectively) as we had expected (see Fig. 13). It was also observed that topology-based methods did not perform well for rectangular prismatic parts especially at medium and low recall values. However, for many of these categories the view-based methods yielded better results, except for two categories ‘slender links’ and ‘bearing blocks’. While the internal contour details negatively affect the view-based methods for these categories, the LFD method overcomes the disadvantages by focusing only on the external silhouette, thereby leading to much higher precision.

4.2.3. Solids of revolution

The PR curves for the Solids of Revolution super-class is shown in Fig. 14. Although many shapes in this category contain many internal features, the external shape is distinct for these classes. For example, all the view-based methods (LFD, 2.5D SH, and 2D SD) performed significantly better than the other methods for this class. Similarly, the 3DSH and CHH techniques performed better than 3DSD.

4.2.4. PRCs for individual classes

In this section, we will discuss in further detail the performance of various methods for particular shape categories having unique, non-standard parts. This analysis gives us a

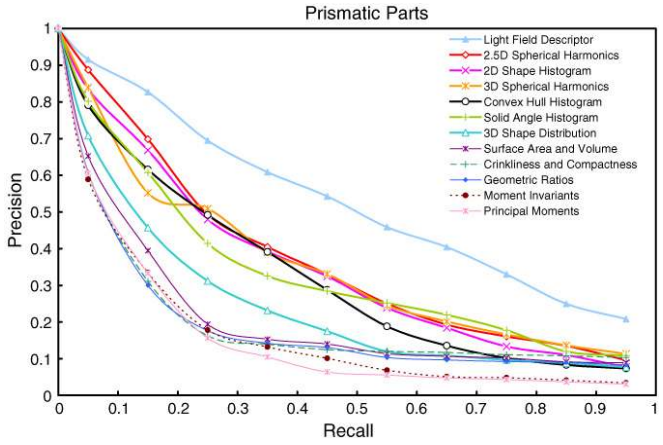

Fig. 13. Precision–recall curves for prismatic parts.

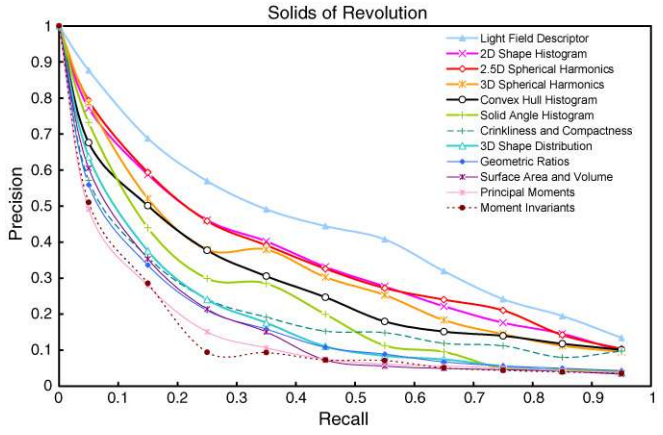

Fig. 14. Precision–recall curves for solids of revolution.

picture of the behavior of different shape representations in a typical engineering scenario. We have presented results from six shape categories representing two from each super-class.

Contact switches (Flat-thin walled parts)

All parts in this class have a common feature – the rectangular slot – which is related to its function as a contact switch. The SAV method seems to capture the shape content better than the other methods. This is due to the fact that most of these components have a very small uniform thickness. Due to the variations in the overall shape like presence of bends and different aspect ratios, the statistics-based and view-based methods show a drop in performance for after a recall of 0.2 (see Fig. 15), indicating that they are able to identify the closest shapes based on overall similarity, but not the other shapes in this category. We suspect that methods based on feature detection and other topology-based methods can capture this common feature fairly well. This class highlights the fact that an ideal search system should not only consider the overall shape, but also allow search based on individual design features. Simple shape measures such as the SAV can be used in these cases to prune the search space quickly.

Brackets (Flat-thin walled parts)

From Fig. 16, all methods perform similarly for this class. The statistics-based and the view-based methods perform poorly for this category. The performance of all the methods is poor, mainly due to the fact that the variety in shapes is significant. The distinguishing characteristic of this category is the small thickness and the bends. We expected the SAV and CC methods to perform well on this category, but these measures are too simple to distinguish shapes from other categories which may have similar surface area and volume but different shape features.

Motor bodies (Prismatic parts)

The parts in this category are solid and have comparable dimensions along the three axes. Hence the 3D Spherical Harmonics and Shape Histogram methods perform well for this category. The view-based methods also perform well for this category, as seen in Fig. 17. Although all the models in this category look similar, the individual design features are located in different positions making each object distinct from the other. Due to the minor variations in design features, this category is especially challenging for view-based methods because many parts in the database will have a similar silhouette. It is therefore

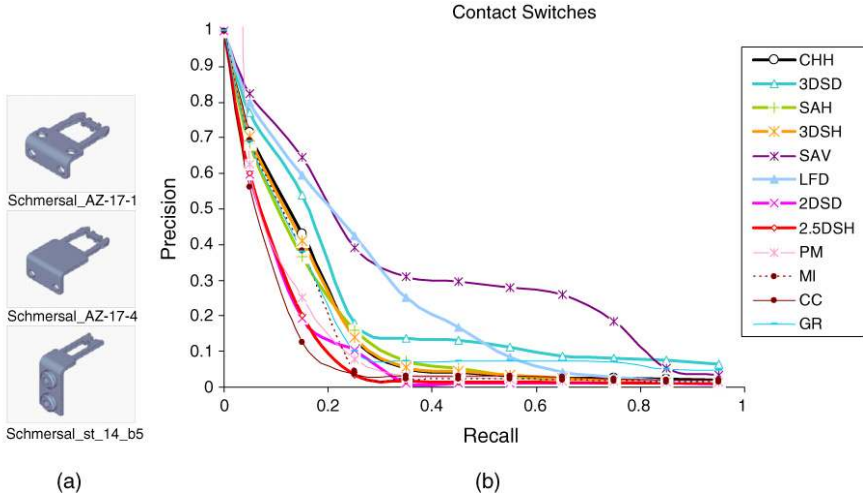

Fig. 15. Contact switches — (a) Sample parts, (b) PRC.

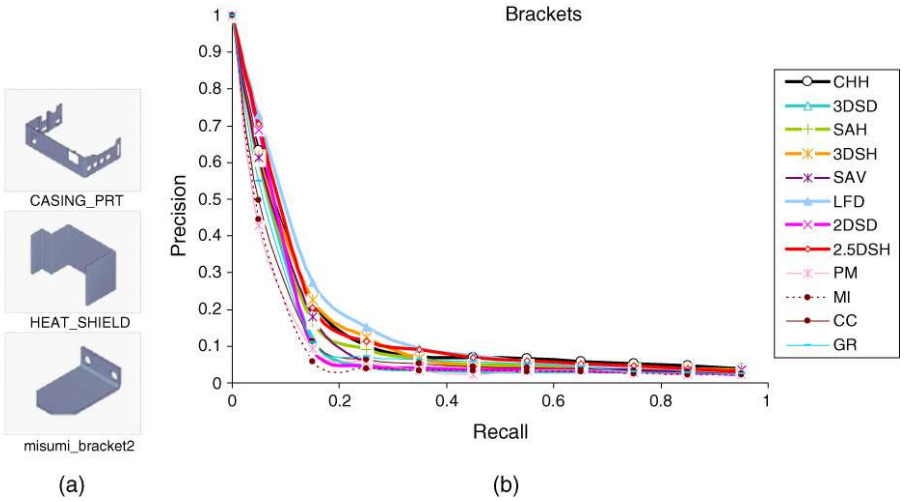

Fig. 16. Bracket-like parts — (a) Sample parts, (b) PRC.

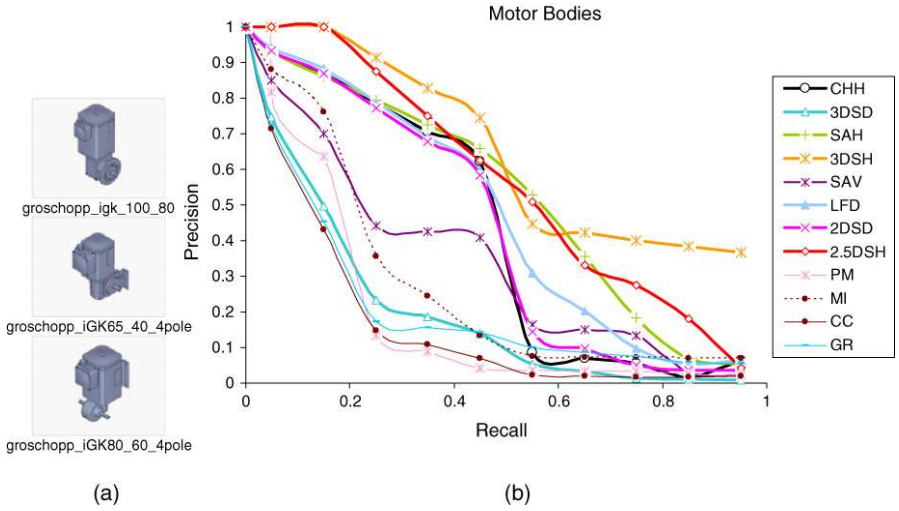

Fig. 17. Motor bodies — (a) Sample parts, (b) PRC.

not surprising that SAH and 3DSH methods perform better than the view-based methods because they consider the complete 3D shape rather than just the views. Since the 2.5DSH method captures the internal details of view in its representation, it performs better than LFD. The sudden drop in precision for 2DSD, LFD, and CHH methods after a recall of 0.5 is due to the fact that four of the seven models are more similar to each other than the others, especially the outer envelope.

U-shaped parts (Prismatic parts)

Only the LFD and SAH methods performed well for this category, suggesting that the other methods did not capture the essential features — the main stem and appendages on both ends (Fig. 18). The other two view-based methods – 2.5DSH and 2DSD – do not perform well due to the pose estimation procedure adopted prior to computing the shape representations. While these methods use three orthogonal views, LFD overcomes this limitation by taking many more views. On the other hand, the SAH method performed well for this category because the essential shape is captured in the axis-parallel bins of the shape histogram.

Spoked wheels (Solids of revolution)

The essential shape features of this category are the radial spokes connected to the external rim of the wheels. LFD performs better than the other view-based methods because in addition to the contour it also retains the region-based information. This captures the spokes and the gaps between them. From Fig. 19, it is noted that SAH and 3DSH perform better than the remaining methods. The SAH particularly captures the distributed features on the rim in the axis-parallel bins enabling it to perform better.

Non-90 degree elbows (Solids of revolution)

The two spherical harmonics method (3DSH and 2.5DSH) perform remarkably well for this category, as can be seen in Fig. 20. These methods perform nearly perfect, suggesting that they can capture the elongated, tubular nature of these parts. Although 2DSD and LFD are also view-based methods, they do not perform as well as the 2.5DSH method. On the other hand, the CHH method performs well initially but loses precision for higher recall.

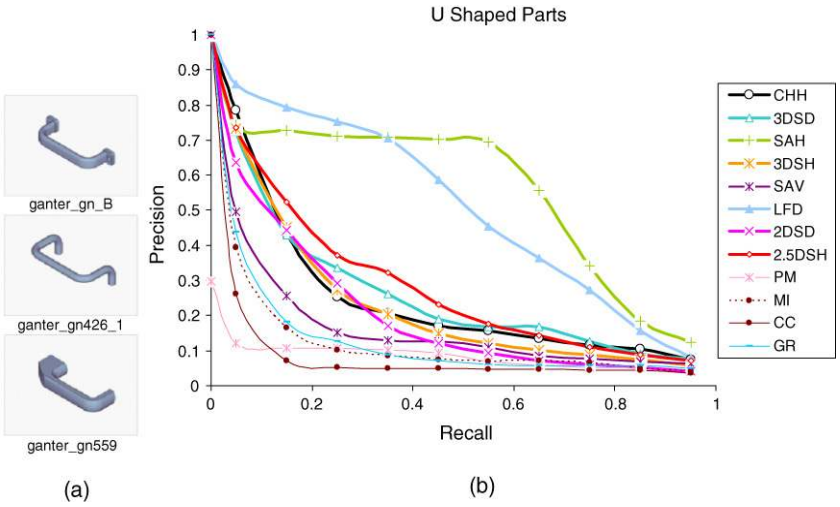

Fig. 18. U-shaped parts — (a) Sample parts, (b) PRC.

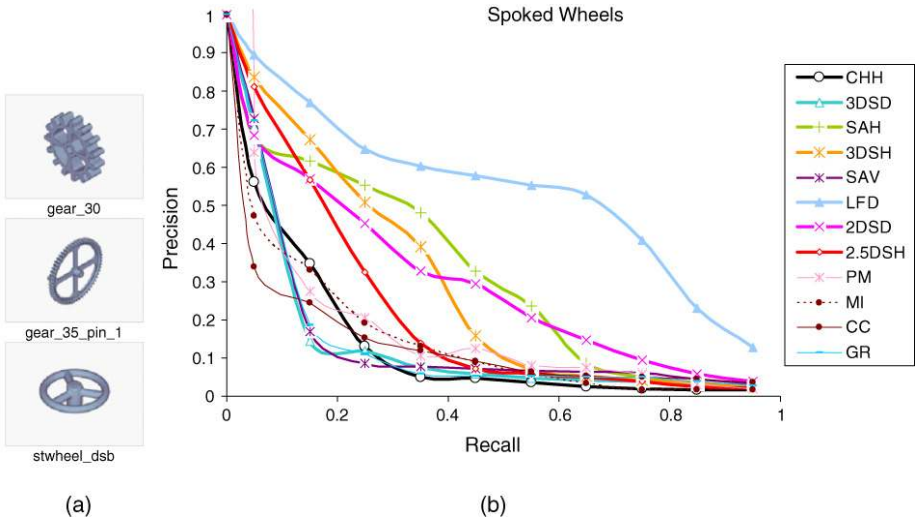

Fig. 19. Spoked wheels — (a) Sample parts, (b) PRC.

4.3. Summary of results

Comparing the results from AAD and ESB, it is clear that, in general, the view-based methods tend to perform well for all the classifications. The LFD method performed best for all the classifications except for the AAD manufacturing classification. The other two view-based methods – 2.5DSH and 2DSD – provided better precision for the manufacturing classification and performed better than other shape representations.

From the results for individual classes, it was found that no single method performs well on all categories. It is also evident that different methods have different strengths and weaknesses. Sometimes, even simple measures such as SAV and CC can be used as quick and approximate filters for certain types of shapes.

5. Conclusions

In the engineering domain, it is important to analyze which shape representations perform well for a particular part category, a view that may seem contrary to the views of researchers in computer vision and graphics. Such analysis and understanding can lead to development of better representations.

In summary, we have developed a publicly available engineering shape benchmark (ESB) for comparing various shape-based search algorithms. ESB includes a set of 867 models in two neutral formats (STL and OBJ) along with associated JPG images and a classification schema. All this data is available from our website http://purdue.edu/shapelab.

The main contributions of this paper are: (1) development of a new, elaborate engineering shape benchmark, (2) evaluation of several shape representations on the benchmark datasets in the engineering domain, the ESB and AAD, and (3) an understanding of the effectiveness of 12 different shape representations across several classes of engineering parts. We used D2 shape distributions (3DSD) as a base method to evaluate the performance of other methods on the ESB. It was found that, among all the methods tested, the three view-based shape representations, viz., LFD, 2.5DSH and 2DSD,

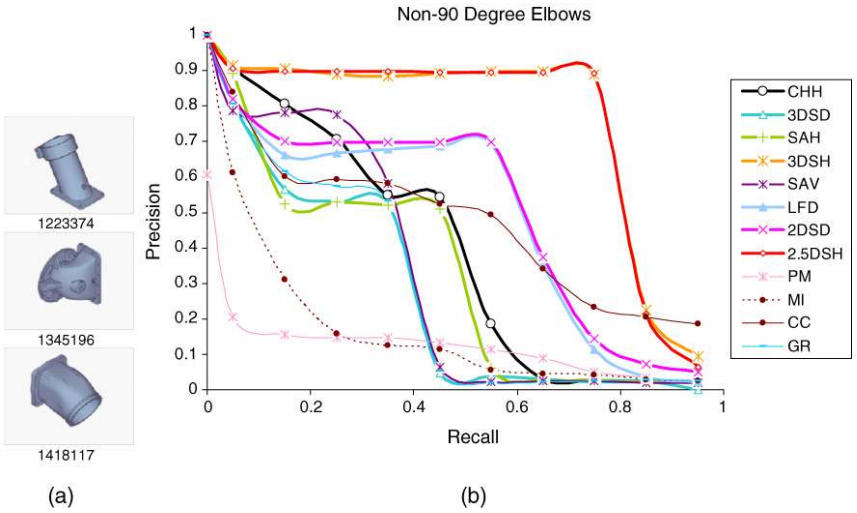

Fig. 20. Non-90 degree elbows — (a) Sample parts, (b) PRC.

perform better than other 3D shape-based methods except for the LEGO® dataset.

The better performance of 2D view-based algorithms for all classes of shapes in the ESB reinforces our intuition that engineering shapes exhibit distinguishing shape features in their 2D views. In addition, 3D spherical harmonics seem to perform reasonably well for the prismatic parts and solids of revolutions compared to other shape representations. Similarly, shape histograms based on solid angles (SAH) performed well on the LEGO dataset. Although many of the 3D shape representations cannot be directly applied to 2D drawings, most of the view-based representations can be applied for 2D–2D or 2D–3D matching as well.

While the task of classification is difficult, to the best of our knowledge, this is the most extensive effort at creating a benchmark database for engineering shapes encompassing a large number of classes and comparing shape representation methods. We will continue to add models to the ESB with contributions from the research community, to encompass a wider variety of shapes so that researchers can conduct detailed studies regarding the performance of shape representations across the whole spectrum of engineering shapes. We expect that our efforts at building the ESB and conducting studies using ESB for classes of engineering shapes will give rise to more robust shape representations.

Acknowledgments

We would like to thank the anonymous reviewers for their suggestions leading to an improved manuscript. The initial funding for this project came from the 21st Century Research and Technology Fund award from the state of Indiana. We acknowledge Professor Karthik Ramani's University Faculty Scholar award from Purdue University, which seeded this project. Supplemental support from the e-Enterprise Center and Center for Advanced Manufacturing at Discovery Park, Purdue University is acknowledged. The implementation of various methods by Alok Bhide and Josh Olsen deserves special mention.

References

[1] Pope A. Model-Based object recognition: A survey of recent research. Technical report 94-04. Canada: Department of Computer Science, University of British Columbia; 1994.

[2] Rowe J, Razdan A, Collins D, Panchanathan S. A 3D digital library system: Capture, analysis, query, and display. In: Proceedings of 4th international conference on digital libraries. 2001.

[3] Kastenmüller G, Kriegel H-P, Seidl T. Similarity search in 3D protein databases. In: Proceedings of German conference on bioinformatics. 1998.

[4] Bruno IJ, Kemp NM, Artymiuk PJ, Willett P. Representation and searching of carbohydrate structures using graph-theoretic techniques. Carbohydrate Research 1997;304:61–7.

[5] Tangelder J, Veltkamp RC. A survey of content based 3D shape retrieval methods. In: Proceedings of shape modeling international. 2004. p. 145–56.

[6] Iyer N, Jayanti S, Lou K, Kalyanaraman Y, Ramani K. Three-dimensional shape searching: State-of-the-art review and future trends. Computer Aided Design 2005;37(5):509–30.

[7] Cardone A, Gupta SK, Karnik M. A survey of shape similarity assessment algorithms for product design and manufacturing applications. ASME Journal of Computing and Information Science in Engineering 2003;3(2): 109–18.

[8] McWherter D, Regli WC. An approach to indexing databases of solid models. Technical report DU-MCS-01-02. Philadelphia (PA): Drexel University; 2001.

[9] Iyer N, Kalyanaraman Y, Lou K, Jayanti S, Ramani K. A reconfigurable 3D engineering shape search system part I: Shape representation. In: Proceedings of ASME DETC 03 computers and information in engineering (CIE) conference. 2003.

[10] Lou K, Jayanti S, Iyer N, Kalyanaraman Y, Ramani K, Prabhakar S. A reconfigurable 3D engineering shape search system part II: Database indexing, retrieval and clustering. In: Proceedings of ASME DETC 03 computers and information in engineering (CIE) conference. 2003.

[11] Foster C, Hayes E, Ip CY, McWherter D, Peabody M, Shapirsteyn Y, et al. National design repository project: A status report. In: International joint conferences on artificial intelligence (IJCAI) and AAAI/SIGMAN workshop on AI in manufacturing systems. 2001.

[12] McWherter D, Peabody M, Regli WC, Shoukofandeh A. An approach to indexing databases of graphs. Technical report DU-MCS-01-01. Philadelphia (PA): Department of Mathematical and Computer Science, Drexel University; June 2001.

[13] Rea H, Corney J, Clark D, Pritchard J, Breaks M, MacLeod R. Part sourcing in a global market. In: Proceedings of ICeCE' 01. Beijing: China Machine Press; 2001.

[14] Corney JC, Rea HJ, Clark DER, Pritchard J, MacLeod RA, Breaks ML. Coarse filters for shape matching. IEEE Computer Graphics and Applications 2002;22(3):65–74.
[15] Cybenko G, Bhasin A, Cohen K. Pattern recognition of 3D CAD objects. Smart Engineering Systems Design 1997;1:1–13.
[16] Kriegel H-P, Kröger P, Mashael Z, Pfeifle M, Pötke M, Seidl S. Effective similarity search on Voxelized CAD objects. In: Proceedings of 8th international conference on database systems for advanced applications. 2003. p. 27–36.
[17] Kriegel H-P, Brecheisen S, Kröger P, Pfeifle M, Schubert M. Using sets of feature vectors for similarity search on voxelized CAD objects. In: Proceedings of ACM SIGMOD int. conf. on management of data. 2003. p. 587–98.
[18] Bespalov D, Regli WC, Shokoufandeh A. Reeb Graph based shape retrieval for CAD. In: Proceedings of ASME design engineering technical conferences, Computers and information in engineering conference, 2003.
[19] Ip C-Y, Lapadat D, Sieger L, Regli WC. Using shape distributions to compare solid models. In: 7th ACM/SIGGRAPH symposium on solid modeling and applications. 2002. p. 273–80.
[20] Shilane P, Min P, Kazhdan M, Funkhouser T. The Princeton shape Benchmark. In: Proceedings of shape modeling international. 2004. p. 167–78.
[21] Hilaga M, Shinagawa Y, Kohmura T, Kunii TL. Topology matching for fully automatic similarity estimation of 3D shapes. In: SIGGRAPH 2001. ACM Press; 2001. p. 203–12.
[22] Kazhdan M, Funkhouser T, Rusinkiewicz S. Rotation invariant spherical harmonic representation of 3D shape descriptors. In: Proceedings of ACM/Eurographics symposium on geometry processing. 2003. p. 167–75.
[23] Jiantao P, Ramani K. A 3D model retrieval method using 2D freehand sketches. In: Fourth international workshop on computer graphics and geometric modeling. 2005.
[24] Jiantao P, Lou K, Ramani K. A 2D Sketch user interface for 3D CAD model retrieval. In: Proc. of CAD'05. 2005.
[25] Osada R, Funkhouser T, Chazelle B, Dobkin D. Shape distributions. ACM Transactions on Graphics 2002;21(4):807–32.
[26] Barber BC, Dobkin D, Huhdanpaa H. The Quickhull algorithm for convex hulls. ACM Transactions on Mathematical Software 1996;22(4):469–83.
[27] Boutin M, Kemper G. On graph matching. PRECISE technical report. PRE-TR-2004-1, West Lafayette (IN): Purdue University; 2004.
[28] Kalyanaraman Y, Boutin M, Ramani K. Effectiveness of convex hull histograms for shape matching. PRECISE technical report. PRE-TR-2005-2, West Lafayette (IN): Purdue University; 2005.
[29] http://www.designrepository.org.
[30] http://www.part-solutions.com/.
[31] http://www.traceparts.com.
[32] Swift KG, Booker JD. Process selection — from design to manufacture. NY: John Wiley and Sons; 1998.
[33] Proceedings of the thirteenth text retrieval conference. 2004. http://trec.nist.gov/pubs/trec13/appendices/CE.MEASURES.pdf.
[34] Sotzio A, Shamir A. Feature sensitive 3D shape matching. In: Proceedings computer graphics international. 2004. p. 596–99.
[35] Demirci M, Shokoufandeh A, Dickinson S, Keselman Y, Bretzner L. Many-to-many feature matching using spherical coding of directed graphs. In: Proceedings of European conference on computer vision, 2004.
[36] Reeb G. Sur les Points Singuliers d'une Forme de Pfaff Completement Integrable ou d'une Fonction Numerique (On the singular points of a completely integrable Pfaff form or of a numerical function). Comptes Randusde l'Academie Sciences Paris 1946;222:847–9.
[37] Hilaga M, Shinagawa Y, Kohmura T, Kunii TL. Topology matching for fully automatic similarity estimation of 3D shapes. In: SIGGRAPH. ACM Press; 2001. p. 203–12.
[38] Chen D-Y, Ouhyoung M. A 3D object retrieval system based on multi-resolution Reeb graph. In: Proceedings of computer graphics workshop. 2002. p. 16.
[39] Bespalov D, Regli WC, Shokoufandeh A. Reeb graph-based shape retrieval for CAD. In: Proceedings of the ASME DETC 03 computers and information in engineering (CIE) conference. 2003.
[40] Iyer N, Jayanti S, Ramani K. An Engineering Shape Benchmark for 3D models. In: Proc. of the ASME IDETC/CIE 2005. 2005.
[41] Bespalov D, Ip CY, Regli WC, Shaffer J. Benchmarking CAD search techniques. In: Proc. of the 2005 ACM symposium on solid and physical modeling. 2005. p. 275–86.
[42] Jiantao P, Ramani K. On visual similarity based 2D drawing retrieval. Computer-Aided Design 2006;38(3):249–59.
[43] Chen D-Y, Ouhyoung M, Tian X-P, Shen Y-T. On visual similarity based 3D model retrieval. Computer Graphics Forum 2003;223–32.
[44] Cyr CM, Kimia BB. 3D object recognition using shape similarity-based aspect graph. In: Proc. of the eighth IEEE international conference on computer vision. vol. 1, 2001 p. 254–61.
[45] Bustos B, KEIM DA, Saupe D, Schreck T, Vranic D. Feature-based similarity search in 3D object databases. ACM Computing Surveys (ÇSUR) 2005;37(4).
[46] Elad M, Tal A, Ar S. Directed search in a 3d objects database using svm. Technical report, Israel: HP Laboratories; 2000.
[47] Elad M, Tal A, Ar S. Content based retrieval of VRML objects—an iterative and interactive approach. In: 6th Europgraphics workshop on multimedia. 2001. p. 107–18.
[48] van Rijsbergn CK. Information retrieval. Butterworths; 1975.
[49] Sadjadi FA, Hall EL. Three-dimensional moment invariants. IEEE Transactions on Pattern Analysis and Machine Intelligence 1980;2(2): 127–36.
[50] Rea HJ, Sung R, Corney JR, Clark DER, Taylor NK. Interpreting three-dimensional shape distributions. IMechE Journal of Mechanical Engineering Science - Part C 2005;219(C6):553–66.
[51] Gombinski J. Industrial classifications and coding. Engineering Materials and Design 1964;7:600–5.
[52] Ullman DG. The mechanical design process. McGraw-Hill; 1992.
[53] http://shapes.aim-at-shape.net/.